Bulletin of the Seismological Society of America, Vol 72, No 2, pp 491-506, April 1982

INVERSION OF COMPLEX BODY WAVES

By Masayuki Kikuchi* and Hiroo Kanamori

ABSTRACT

A numerical method to deconvolve complex body waves into a multiple shock sequence is developed. With the assumption that all the constituent events of a multiple shock have identical fault geometry and depth, the far-field source time function is obtained as a superposition of ramp functions. The height and the onset time of the ramp functions are determined by matching the synthetic waveforms with the observed ones in the least-square sense.

The individual events are then identified by pairs of ramp functions or discrete trapezoidal pulses in the source time sequence. The method can be used for the analysis of both single and multi-station data. Teleseismic long-period *P* waves from the 1976 Guatemala earthquake are analyzed as a test of our method. The present method provides a useful tool for a systematic analysis of multiple event sequences.

Introduction

The spectra and waveforms of seismic body waves provide important information on the details of the source rupture process. In frequency domain analysis, the low-frequency asymptote and the corner frequency of the displacement spectrum are used to estimate the seismic moment and the source dimension (Brune, 1970). In time-domain analysis of body waves, the observed waveforms are modeled by a source time function, and the time constants associated with it are interpreted in terms of the source dimension and the particle velocity of the fault motion (Aki, 1968; Haskell, 1969; Kanamori, 1972; Abe, 1974).

When the observed body waveforms are relatively simple, the modeling can be done by using either forward or inverse methods. Langston (1976) and Burdick and Mellman (1976) used a time-domain inversion method to determine some of the complexities of the source time function. For a very large earthquake, however, the body waveform is extremely complex, and no standard method is available for the inversion. Several attempts have been made to explain the complexity of body waves from large earthquakes by using a multiple event model. Earlier attempts consisted of identifying distinct phases in the body-wave signal as the beginning of distinct events and locating them with respect to the first one (Imamura, 1937, p. 267; Miyamura *et al.*, 1964; Wyss and Brune, 1967). In more recent studies, synthetic seismograms were used to make a more quantitative interpretation (Fukao, 1972; Chung and Kanamori, 1976). Kanamori and Stewart (1978) modeled the waveforms of *P* waves from the 1976 Guatemala earthquake by matching them, in the least-square sense, with a series of trapezoidal source time functions. Rial (1978) modeled the Caracas earthquake by using three distinct events. Boatwright (1980) employed a direct inversion of the body waves from the 1979 St. Elias, Alaska, earthquake to resolve a few subevents.

The complexity of the source time function reflects the heterogeneity in the mechanical properties in the fault zone, which is often characterized by asperities or barriers. Many recent studies have suggested the importance of asperities in various seismological problems, such as the nature of strong ground motion (Das and Aki,

*Present address. Physics Department, Yokohama City University, Yokohama 236, Japan.

1977; Ebel and Helmberger, 1981), foreshocks (Jones and Molnar, 1979), seismicity patterns (Wesson and Ellsworth, 1973; Kanamori, 1981), and the regional variation of rupture mode (Lay and Kanamori, 1981).

In view of this importance, it is desirable to develop a systematic method for inversion of complex body waves consisting of contributions from several sources. This is obviously a difficult problem. For example, the 1976 Guatemala earthquake was modeled by about 10 pulses, each representing a distinct seismic source. Even in the simplest source model, about six parameters [the seismic moment, three fault parameters, two time constants (e.g., rise time and pulse width)] are necessary to describe each source. Thus, if we are to model a multiple shock with 10 distinct events, about 100 parameters, including the origin time and the coordinates of the individual events, would have to be determined. In view of the amount, the quality and the limited bandwidth of the data usually available for this type of modeling, it would be very difficult to determine all of the parameters. Furthermore, in view of the complexity of the structure near the source, along the path, and near the receiver, it would not be easy to prove that all the complexities in the body wave form are due to the source.

Because of these difficulties, we will be mainly concerned with the gross complexities of multiple events rather than with the minute details of the source function, and a number of simplifications will be made. Inevitably, a certain amount of nonuniqueness and subjectivity exists. The validity of the model should eventually be judged in the light of other data such as local strong-motion data, distribution and geometry of surface breaks, and macroseismic data. As we will show in the later sections, the method we present here can invert complex observed seismograms into a source time function in a systematic and reasonably objective way, thereby providing a means for interpreting complex observed records in terms of asperities and barriers in the fault zone.

Method

In an infinite homogeneous space, the far-field body waveform due to a shear dislocation source is given by [e.g., (10) in Haskell, 1964]

$$U_c(\vec{x}, t) = \frac{R_c \mu}{4\pi\rho c^3 r_0} \int\int_A \dot{D}(\vec{\xi}, t - r/c)\, dA \tag{1}$$

where A = dislocation surface, $\vec{\xi}$ = a variable point on A, $\vec{x}$ = an observation point, t = time, $r = |\vec{x} - \vec{\xi}|$, r_0 = the average of r, $\dot{D}(\vec{\xi}, t)$ = relative slip velocity, R_c = radiation pattern, ρ = density, μ = rigidity, and c = body-wave velocity.

When the source region is small, the travel time r/c in (1) can be approximated by its average, r_0/c. The waveform is then given by

$$U_c(\vec{x}, t) = \frac{R_c}{4\pi\rho c^3 r_0} S(t - r_0/c) \tag{2}$$

where $S(t)$ is the far-field source time function defined by

$$S(t) = \mu \int\int_A \dot{D}(\vec{\xi}, t)\, dA. \tag{3}$$

Here we assume that the time history of dislocation at a point is given by a

function of the time measured from the arrival of a rupture front. Let $t'(\vec{\xi})$ be the arrival time at a point $\vec{\xi}$, then the dislocation function is expressed as

$$D(\vec{\xi}, t) = D(t - t'(\vec{\xi})). \tag{4}$$

Noting that $dA = (dA/dt')\, dt'$ is the area swept by the rupture front during the time interval dt', we can write equation (3) as

$$S(t) = \mu \int_0^\infty \dot{D}(t - t')\dot{A}(t')\, dt' \tag{5}$$

where dot denotes the time derivative. Thus the far-field source time function is expressed by a convolution of the dislocation velocity and the fault area expansion rate.

We assume that the disolcation time history is given by a ramp function with rise time τ as

$$D(t) = D_0 s(t)$$

where D_0 is the final dislocation and $s(t)$ is the unit ramp function

$$s(t) = \begin{cases} 0 & t < 0 \\ t/\tau & 0 \leqq t \leqq \tau. \\ 1 & t > \tau \end{cases}$$

If rupture propagation is characterized by abrupt changes of the fault area expansion rate, then

$$\dot{A}(t) = \sum_i \Delta\dot{A}_i H(t - t_i) \tag{6}$$

where $\Delta\dot{A}_i$ is the increment of the fault area expansion rate at time t_i, and $H(t)$ is the Heaviside step function. The source time function $S(t)$ is then given by superposition of ramp functions

$$S(t) = \sum_i m_i s(t - t_i) \tag{7}$$

where

$$m_i = \mu D_0 \Delta\dot{A}_i.$$

For example, in case of unilateral rupture propagation,

$$A = Wvt (0 \leqq t \leqq T)$$

(W = fault width, v = rupture velocity)

and the far-field source time function can be described by a pair of pulses as follows

$$m_1 = \mu W v D_0, \quad t_1 = 0, \quad m_2 = -\mu W v D_0, \quad t_2 = T.$$

When these pulses are convolved with $s(t)$, a trapezoidal far-field source time function is produced. In case of asymmetric bilateral rupture,

$$A = 2wvt \quad \text{for} \quad 0 \leqslant t \leqslant T_1$$
$$wvt \quad \text{for} \quad T_1 \leqslant t \leqslant T_2$$

and

$$m_1 = 2\mu WvD_0, \qquad t_1 = 0; \quad m_2 = -\mu WvD_0, \qquad t_2 = T_1;$$
$$m_3 = -\mu WvD_0, \qquad t_3 = T_2.$$

In this representation, a positive and negative m_i indicate the beginning and the end of a discrete rupture, respectively. When an earthquake source consists of multiple events with identical fault orientation and depth, the far-field source time function is given by a superposition of trapezoidal pulses. Then the area under each trapezoid gives the seismic moment of the individual event. The source time function in this case is also described in the form of equation (7), and is used for the analysis of teleseismic body waves from a complex multiple shock. We assume that an earthquake source is expressed as a superposition of point dislocations with identical fault orientation and depth. The fault geometry is assumed to be known from the radiation pattern of body and/or surface waves. The only unknown is the source time function which is sought in the form of a ramp function series.

In the following, we shall restrict ourselves only to P-wave analysis. First we shall treat a record from a single station and then extend the analysis to simultaneous deconvolution of multi-station data.

Single-station data analysis. Let $x(t)$ denote an observed P waveform (vertical component) at a station and $w(t)$ denote a synthetic wavelet corresponding to a unit source ramp function: $s(t)$. In the synthesis of the wavelet, a double-couple point source is placed at a depth in a homogeneous half-space. Then the far-field P-wave seismogram is given as follows (Langston and Helmberger, 1975; Kanamori and Stewart, 1976)

$$w(t) = \frac{R_{pz}}{4\pi\rho\alpha^3}\left(\frac{1}{r_0}\right)[s(t) + R_{p^P}s(t - \Delta t_{p^P}) + \frac{\eta_\alpha}{\eta_\beta}R_{s^P}s(t - \Delta t_{s^P})]*Q(t)*I(t) \tag{8}$$

where the time is measured from the initial arrival of P wave, $(1/r_0)$ denotes the effective geometrical spreading, and the notation for other parameters is the same as in Langston and Helmberger (1975). As a first approximation, the rise time τ is estimated by comparing the synthetic wavelet to the initial portion of the observed waveform.

First we take a single wavelet and determine m_1 and t_1 by minimizing the error defined by

$$\Delta_1 = \int_0^\infty [x(t) - m_1 w(t - t_1)]^2\, dt. \tag{9}$$

Equation (9) can be written in terms of correlation functions as follows

$$\Delta_1 = r_x(0) - 2r_{wx}(t_1)m_1 + r_w(0)m_1^2 \tag{10}$$

where

$$r_x(t') = \int_0^\infty x(t)x(t+t')\,dt$$

$$r_{wx}(t') = \int_0^\infty w(t)x(t+t')\,dt$$

$$r_w(t') = \int_0^\infty w(t)w(t+t')\,dt. \tag{11}$$

The right-hand side of equation (10) has a quadratic form with respect to m_1. Since $r_w(0)$ is positive, Δ_1 is minimized if

$$\partial\Delta_1/\partial m_1 = 0 \quad \text{or} \quad m_1 = r_{wx}(t_1)/r_w(0). \tag{12}$$

For this value of m_1,

$$\Delta_1 = r_x(0) - r_w(0)m_1^2. \tag{13}$$

From equation (13) we find that Δ_1 is minimized if the onset time t_1 is chosen so that

$$[r_{wx}(t_1)]^2 = \text{maximum}. \tag{14}$$

Next we apply the above procedure to the residual waveform

$$x'(t) = x(t) - m_1 w(t - t_1). \tag{15}$$

Then the values of t_2 and m_2 for the second wavelet are determined by minimizing $[r_{wx}(t_2)]^2$ and by

$$m_2 = r_{wx}(t_2)/r_w(0).$$

The above procedure is iterated until no more significant decrease in the error occurs. After N iterations, the N largest m_i's and the corresponding t_i's are obtained, and the source time function $S(t)$ can be calculated by equation (7). Also the synthetic waveform $y(t)$ and the approximation error are obtained by

$$y(t) = \sum_{i=1}^{N} m_i w(t - t_i) \tag{16}$$

$$\Delta_N = \int_0^\infty [x(t) - y(t)]^2\,dt$$

$$= r_x(0) - r_w(0)\left[\sum_{i=1}^{N} m_i^2\right]. \tag{17}$$

It should be noted here that, if the number of iterations N is fixed, the approximation error Δ_N can be regarded as a function of the rise time τ used in the synthesis of the wavelet. Hence, after some trial and error, we adjust the value of τ so that it minimizes Δ_N.

Multi-station data analysis. A similar method can be used for the analysis of multi-station data. However, if the source location differs from event to event in a multiple shock sequence, the relative arrival times of these events with respect to the first event are different from station to station. It is therefore necessary to introduce the source location as an additional parameter. This requires a slight modification of the single-station method described above.

Here we shall consider a multiple shock where rupture occurs along a relatively narrow fault plane. Let W be the fault width and l be the distance along the fault strike measured from a reference point. Considering the dependence of the travel time on the location of a shear dislocation source, we write equation (1) as follows

$$u_\alpha(\vec{x}, t) = \frac{R_\alpha}{4\pi\rho\alpha^3 r_0} S_\alpha(t - r_0/\alpha; \Phi) \tag{18}$$

where

$$S_\alpha(t; \Phi) = \mu W \int_0^\infty \bar{\dot{D}}(l, t + l \cos \Phi/\alpha)\, dl \tag{19}$$

$\bar{\dot{D}}$ being the slip velocity averaged over the fault width, the angle between the ray path and the rupture direction. The function $S_\alpha(t; \Phi)$ becomes equivalent to the far-field source time function $S(t)$ defined by (3) if $\Phi = 90°$ or the entire fault length is small enough for $l \cos \Phi/\alpha$ to be neglected.

Using a ramp function for the dislocation time history, we find

$$S_\alpha(t; \Phi) = \mu W D_0 \int_0^\infty \frac{s(t - t' + l \cos \Phi/\alpha)}{1 - v \cos \Phi/\alpha}\, \dot{v}\, dt' \tag{20}$$

where l is the coordinate of the rupture front at time t', and $v = \dot{l}$ is the rupture velocity. Under a condition similar to relation (6), we find an expression for $S_\alpha(t; \Phi)$ as follows

$$S_\alpha(t; \Phi) = \sum_i m_i s(t - t_i + l_i \cos \Phi/\alpha) \tag{21}$$

where

$$m_i = \mu D_0 W \Delta v_i/(1 - v_i \cos \Phi/\alpha). \tag{22}$$

For a shallow earthquake with which we are concerned here,

$$\cos \Phi = \sin i_0 \cos \Delta\phi$$

where i_0 is the take-off angle and $\Delta\phi$ is the angle between the station azimuth and the fault strike. Since we use only stations with the distance $\Delta \geqslant 40°$ and the rupture

velocity v is expected to be less than the shear wave velocity, the azimuth-dependent factor of m_i, $(1 - v \cos \Phi/\alpha)$ can be replaced by 1 as a first-order approximation. Thus the ith source pulse is specified by a set of three parameters: (m_i, t_i, l_i).

Let $x_j(t)$ denote the P waveform observed at jth station and $w_j(t, l)$ denote a synthetic wavelet which is generated by a unit source at a distance l from the reference point and recorded at jth station. Taking the azimuth-dependent time shift $(l \cos \Phi_j/\alpha)$ into account, we write

$$w_j(t; l) = w_j(t + l \cos \Phi_j/\alpha) \tag{23}$$

where $w_j(t) \equiv w_j(t; 0)$ is the function given by (8). Then the first source pulse (m_1, t_1, l_1) can be determined by minimizing the error

$$\Delta_1 = \sum_{j=1}^{M} \int_0^\infty [x_j(t) - m_1 w_j(t - t_1; l_1)]^2 \, dt \tag{24}$$

where M is the number of stations. By using the same procedure as the one used for single-station data, we can determine t_1 and l_1 from

$$[r_{wx}(t_1, l_1)]^2 = \text{maximum} \tag{25}$$

and

$$m_1 = r_{wx}(t_1; l_1)/r_w(0) \tag{26}$$

where r_{wx} and r_w are the sums of correlation functions defined by

$$\begin{aligned} r_{wx}(t'; l) &= \sum_{j=1}^{M} \int_0^\infty [w_j(t; l) x_j(t + t')] \, dt \\ &= \sum_{j=1}^{M} r_{w_j x_j}(t' - l \cos \Phi_j/\alpha) \end{aligned} \tag{27}$$

$$r_w(0) = \sum_{j=1}^{M} \int_0^\infty [w_j(t; l)]^2 \, dt = \sum_{j=1}^{M} r_{w_j}(0). \tag{28}$$

The residual waveforms are then defined by

$$x'_j(t) = x_j(t) - m_1 w_j(t - t_1; l_1) \tag{29}$$

and the same procedure is repeated for $x_j'(t)$ to obtain the second source pulse (m_2, t_2, l_2).

The above procedure is iterated until no significant decrease in the error occurs. After N iterations, the source time function $S(t; 90°)$ can be calculated by equation (7); the synthetic P waveform $y_j(t)$ and the approximation error Δ_N are obtained by

$$y_j(t) = \sum_{i=1}^{N} m_i w_j(t - t_i + l_i \cos \Phi_j/\alpha) \tag{30}$$

$$\Delta_N = \sum_{j=1}^{M} \int_0^{\infty} [x_j(t) - y_j(t)]^2 \, dt$$

$$= r_x(0) - r_w(0) \sum_{i=1}^{N} m_i^2 \tag{31}$$

where

$$r_x(0) = \sum_{j=1}^{M} r_{x_j}(0)$$

$$r_w(0) = \sum_{j=1}^{M} r_{w_j}(0).$$

In the iterations, we need to calculate only the cross-correlation $r_{wx}(t; l)$. For the sake of computation, the coordinate l along the fault strike is discretized. The cross-correlation r_{wx} is then computed at discrete points on the two-dimensional $(t - l)$ plane. In this case, we can use a recursive formula for r_{wx} to facilitate the computation (see Appendix).

Analysis

As a test of our method, we analyzed teleseismic long-period P waves from the Guatemala earthquake, 4 February 1976. The WWSSN records for this event have been already studied in detail by Kanamori and Stewart (1978).

The extent of the surface breaks and the aftershock area indicates that the source of this earthquake is characterized by a long shallow strike-slip fault (Plafker, 1976; Langer *et al.*, 1976). Kanamori and Stewart (1978) analyzed the teleseismic long-period P waves and showed that the earthquake consisted of about 10 distinct events with a total duration of about 2 min. They assumed that the mechanisms of the individual events are the same as the mechanism of the main shock determined by body-wave first motions and long-period surface waves. The same source parameters as those used by Kanamori and Stewart (1978) are used here to synthesize the basic wavelet (i.e., fault strike = N75°E, dip angle = 90°, slip angle = 5°, depth = 5 km).

We first use the record at NUR and examine the convergence of the synthetic waveform to the observed P wave. A double-couple point source is placed at a depth of 5 km in a homogeneous half-space, and the deconvolution was made by using the single-station method.

Figure 1 shows the error Δ_N normalized to $\Delta_0 = r_x(0)$ as a function of N, where the rise time τ is fixed at 4 sec. It can be seen that the error does not decrease significantly after about 20 iterations. Then we vary the rise time τ with N fixed at 20, and seek the value of τ which minimizes the error Δ_{20}. As shown by Figure 2, Δ_{20} is minimized at $\tau = 3$ sec. This value is therefore considered to be the most appropriate for the rise time of the overall source time function.

The sequence of deconvolution iterations is shown in Figure 3. The source time function $S(t)$ thus obtained and the resulting synthetic waveform are shown in Figure 4, a and b. The source time function consists of about five distinct trapezoids.

In the analysis of other records, the same values of N and τ are used. Figure 5 shows the far-field source time functions thus derived from the individual stations,

where a modification is made to remove a linear trend from each source time function.

The linear trend is probably caused by the inadequate response of the recording instrument (WWSSN LP) at long period, and is not meaningful. In fact, we can remove the linear trend from the source time function without changing the

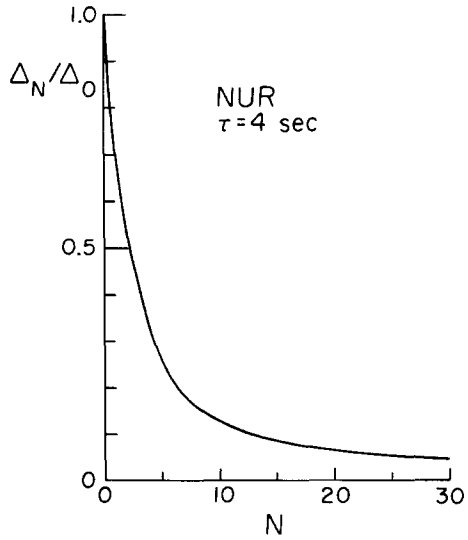

FIG 1 Normalized approximation error, Δ_N/Δ_0 versus iteration N (NUR, the Guatemala earthquake). The rise time τ of ramp functions used for constructing the source time function is fixed at $\tau = 4$ sec

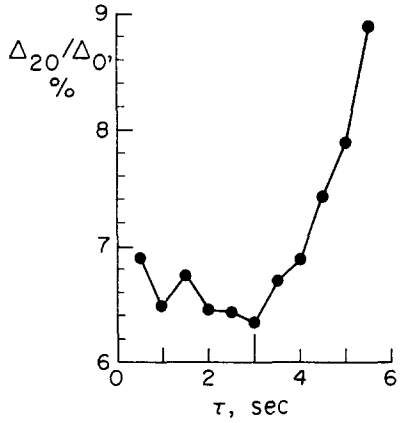

FIG. 2. Normalized approximation error, Δ_{20}/Δ_0 versus the rise time τ (NUR, the Guatemala earthquake). The number of iterations is fixed at $N = 20$.

synthetic waveform significantly. In Figure 6, the synthetic waveforms corresponding to the modified source time functions are shown. The agreement between the synthetic and the observed waveforms is satisfactory. The sequence of the source pulses is very similar from station to station. We can identify five major events as marked in Figure 5. Each of these major events may be divided into subevents. It can be seen that the onset time of the later events (4 and 5) vary in a systematic way as the azimuth of the station changes. This suggests that the later events

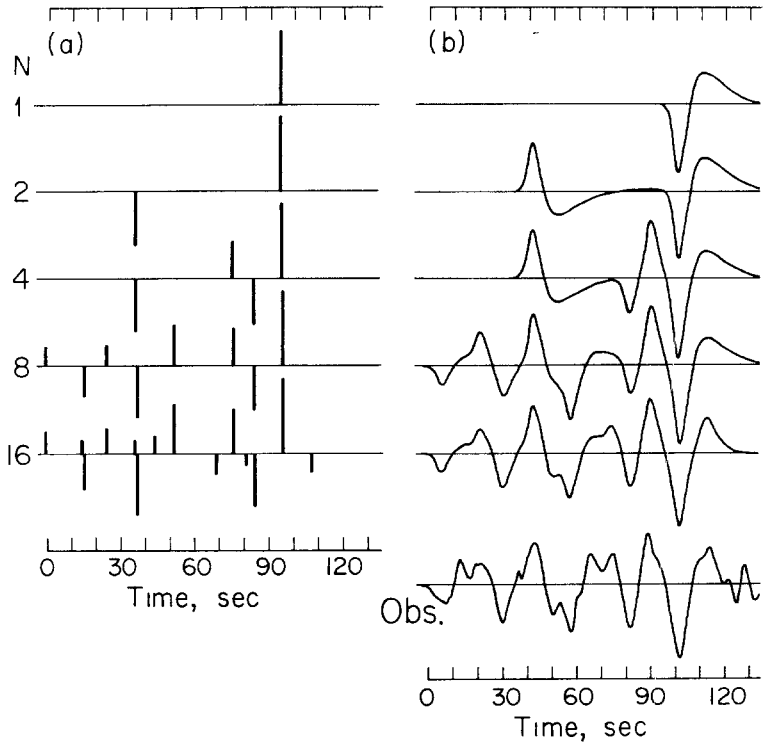

FIG. 3 Sequence of deconvolution procedure in single-station data analysis (NUR, the Guatemala earthquake) (a) source pulses (height of ramp functions); (b) corresponding synthetic waveform. Note that larger pulses are obtained at the earlier steps in the iterations

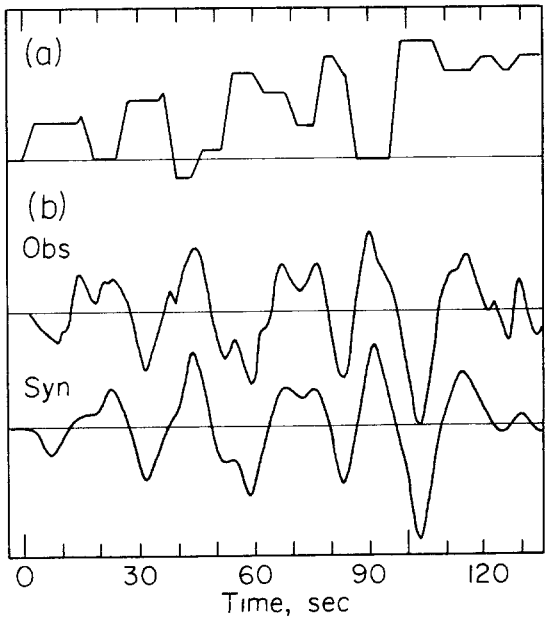

FIG. 4 (a) Far-field source time function obtained after 20 iterations, (b) the resulting synthetic waveform and the observation (NUR, the Guatemala earthquake).

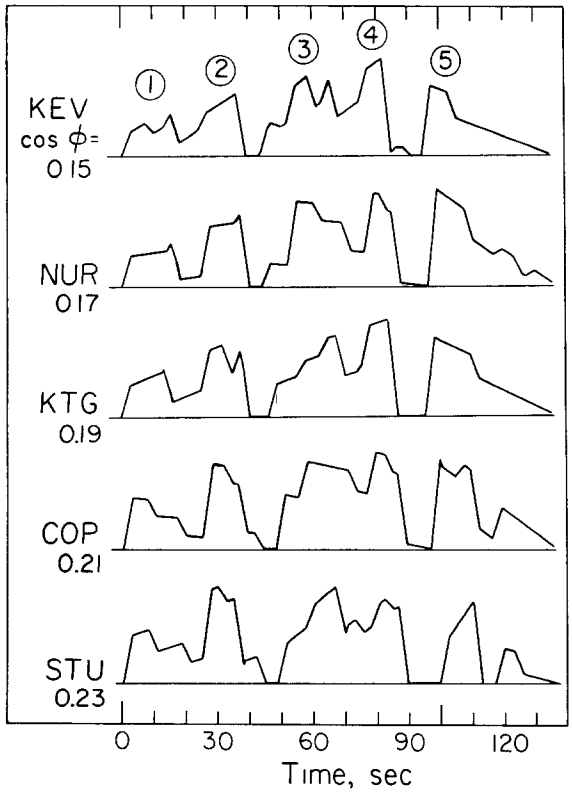

FIG 5. Far-field source time functions obtained from five stations Five major events are identified as marked 1 to 5 by the distinct onset in the time sequences.

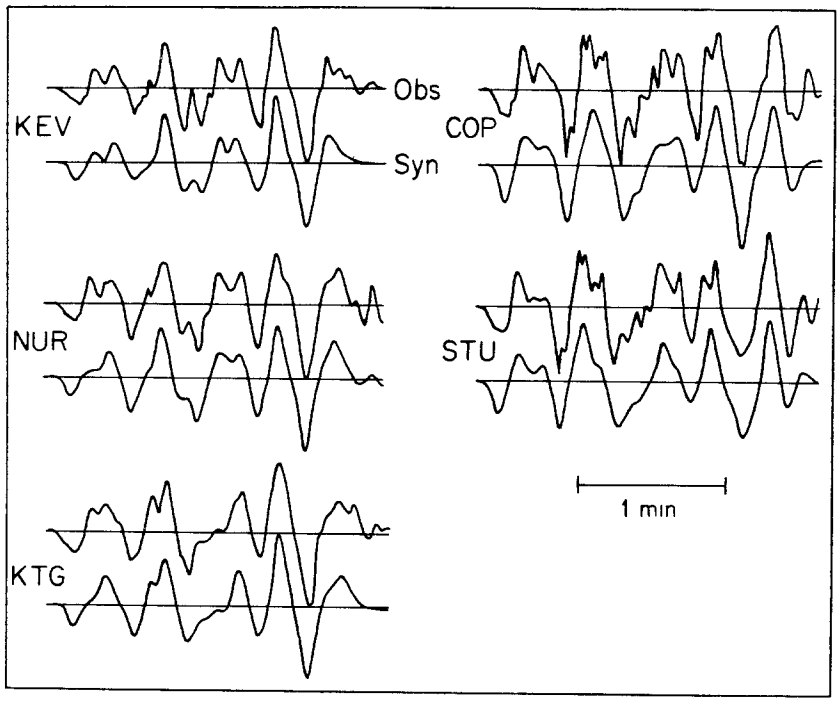

FIG 6. The synthetic waveforms corresponding to the source time functions of Figure 5 are shown in comparison with the observed waveforms

TABLE 1

SEISMIC MOMENT OF INDIVIDUAL EVENTS (UNIT $\times 10^{26}$ DYNE·CM)

Station/ Event	1	2	3	4	5	Total
KEV	5.0	8 8	6.3	9.6	8.0	37.7
NUR	2.3	4.7	7.3	4.4	7.5	26.2
KTG	5 9	3 6	8 4	8.4	7.5	33 8
COP	6.3	7.2	8.8	11.5	5.9	39 7
STU	2.8	8.0	4.9	5.0	7 0	27.7
Mean	4.5	6.5	7.1	7 8	7.2	33 0
Variance	±1.8	±2.2	±1.6	±3.0	±.8	±6.0

$$\sum M_0 = (3.3 \pm 0.6) \times 10^{27} \text{ dyne·cm}$$

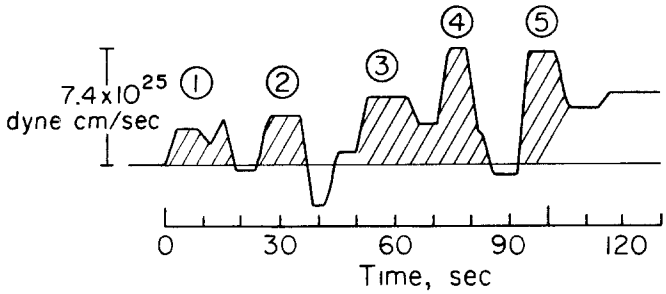

FIG. 7. Far-field source time function, $S(t, 90°)$ obtained by multi-station data analysis (the Guatemala earthquake) Five major events are clearly identified.

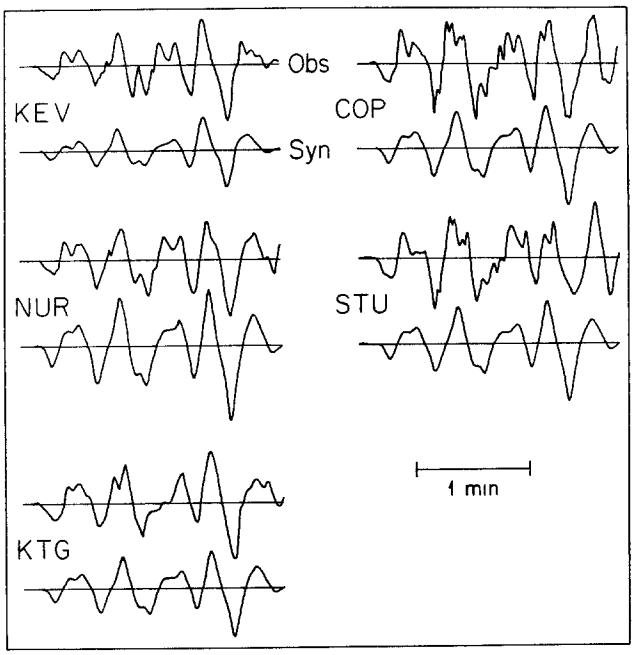

FIG. 8 Synthetic P waveforms corresponding to the source time function of Figure 7 The amplitude scale is the same as that of the observed waveforms at the individual stations

occurred at some distance from the first event. This point will be made clear in the multi-station data analysis as described later.

The seismic moment of the individual events are estimated from the area under the source time function. The results are shown in Table 1. The standard deviation of the seismic moments estimated from different stations is about 30 per cent. The result shown in Table 1 is in good agreement with that obtained by Kanamori and Stewart (1978).

TABLE 2

GUATEMALA EARTHQUAKE

Event	Process Time (sec)	Moment ($\times 10^{26}$ dyne cm)
1	14	4 2
2	11	4.5
3	14	6.4
4	10	6.2
5	10	7.5
Total	59	2.9×10^{27}

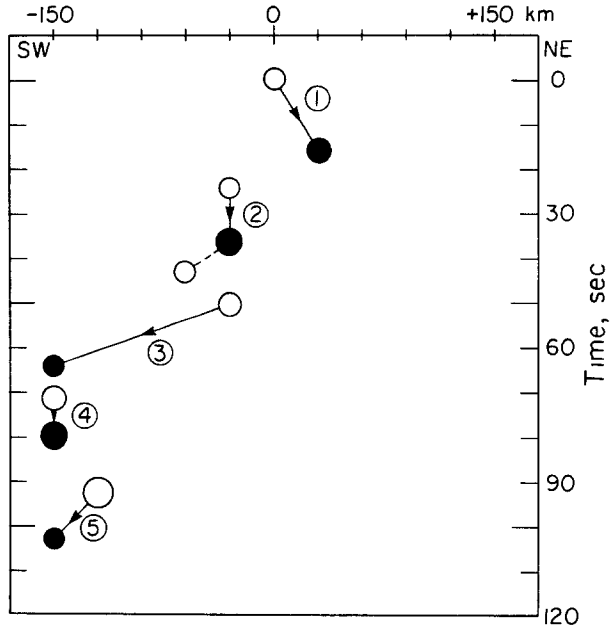

FIG. 9. Location and onset time of 11 largest source pulses obtained by multi-station data analysis (the Guatemala earthquake) Open and closed circles show positive and negative pulses, respectively. Number marked in the figure corresponds to that in Figure 7.

Next, we apply the multi-station method to the same records as used above. We take 11 points, each 30 km apart, along the fault strike as the discrete source locations. The far-field source time function $S(t; 90°)$ thus obtained and the resulting synthetic waveforms are shown in Figures 7 and 8, respectively. The approximation error Δ_{20}/Δ_0 is about 20 per cent. This value is quite satisfactory since it includes the amplitude variation from station to station as well as noise in the records.

Five major events are now clearly identified in the time sequence. The individual process times and seismic moments are shown in Table 2. In Figure 9, the locations

of the larger sources are plotted on the space-time plane, where positive and negative pulses are indicated by solid and open circles, respectively. In event 1, the rupture initiated near the eastern end of the fault and first propagated eastward. Then the rupture propagated primarily westward with a few pauses. Through the sequence from events 1 to 4, almost 180 km of the fault length is ruptured. The total process time is about 50 sec and the mean rupture velocity is about 3.5 km/sec. However almost 30 sec of the total rupture time is spent during the transition from event to event; accordingly, the apparent rupture velocity was about 2 km/sec.

Finally, the largest event occurred near the western end of the fault (event 5). The location obtained suggests that this event occurred along the same fault segment as that of the previous events 3 and 4. Kanamori and Stewart (1978) suggested that the large events in the later stage, which correspond to events 4 and 5 in this paper, are related to the large surface breaks observed near the western end of the fault. This feature is more clearly seen in the present results.

Discussion

In the present study, we assumed that a multiple shock is represented by a series of point dislocations with an identical fault geometry. Once the fault geometry is known, we can calculate the impulse response, namely a wavelet caused by an impulsive point dislocation. The far-field source time function is then obtained by deconvolution of the observed record with the impulse response.

An alternative approach to this problem is to design a linear inverse filter of the impulse response as devised by Levinson (1947). The source time function can be obtained by convolution of this filter with the observed record. The inversion is straightforward since no assumption is needed for the source time function. However, a certain criterion is necessary to identify the individual events. This approach has been used by Strelitz (1980) and Boatwright (1980).

Another method is to parameterize the unknown source time function using a certain number of parameters which characterize the individual events. These parameters are determined by matching the resulting synthetic records with the observed ones (Burdick and Mellman, 1976). In this approach, the identification of the individual events is straightforward, but some assumption about the shape of the source time function (e.g., a triangular source pulse or a trapezoidal pulse) is needed to start the analysis.

It should be noted that, in any method, the far-field source time function $S(t)$ can in principle be determined uniquely for a given source geometry while the identification of the event is somewhat arbitrary. In other words, the same $S(t)$ can be decomposed into a different series of discrete events.

Our approach is a hybrid of the two approaches described above. The far-field source time function is expressed as a superposition of ramp functions with an identical rise time. In this sense, the source time function is parameterized. On the other hand we do not specify the shape of the individual events during the analysis. In this sense, our method is similar to the direct inversion method.

In the single-station data analysis, the far-field source time functions are derived from the individual stations. Multiple events are then identified as discrete pulses which should be identical for all the stations if the events have the same fault mechanism as used for the analysis. The validity of the model can therefore be tested by the similarity of all the source time sequences. In the multi-station data analysis, on the other hand, a single source time function is derived from the multi-station records. In this case, the quality of the model can be measured by how well the synthetic seismograms match the data.

In the present paper, the fault mechanism is assumed to be the same for all the events of a multiple shock. This is probably a reasonable assumption for most events, but there may be cases where substantial changes in the mechanism occur during the sequence. If the change is very drastic, it is possible to detect it by examining the result obtained by the single-station method. If the mechanism of an event is different from the one assumed, the polarity and the amplitude of the source-time function corresponding to it vary substantially from station to station. If the azimuthal coverage of the station is relatively complete, a more appropriate mechanism for that event may be obtained from the polarity and the amplitude variations.

As demonstrated in the earlier section, even a complex event such as the 1976 Guatemala earthquake can be analyzed in a systematic way. Since the Guatemala earthquake is probably one of the most complex strike-slip events, the method presented here provides a useful tool for the analysis of other complex events.

Acknowledgments

We thank John Cipar, Jeffrey Given, Thorne Lay, Larry Ruff, and Fumiko Tajima for useful comments on the manuscript.

This research was supported by the Division of Earth Sciences, National Science Foundation Grant EAR78-11973 and U S. Geological Survey Contract 14-08-0001-19265 and 14-08-0001-19270.

Appendix: Recursive Formula for R_{wx}

Since a single-station record can be regarded as a limit of multi-station records, we here consider only the multi-station data. After the first source pulse (m_1, t_1, l_1) is determined, the residual waveforms are given by

$$x_j'(t) = x_j(t) - m_1 w_j(t - t_1; l_1). \tag{A1}$$

Taking the cross-correlation of $w_j(t; l)$ with $x_j'(t)$, we have

$$\begin{aligned} r_{w_j}{}'x_j(t'; l) &\equiv \int_0^\infty [w_j(t; l)x_j'(t + t')]\, dt \\ &= \int_0^\infty [w_j(t; l)x_j(t + t')]\, dt \\ &\quad - m_1 \int_0^\infty [w_j(t; l)w_j(t + t' - t_1; l_1)]\, dt \\ &= r_{w_j x_j}(t'; l) - m_1 r_{w_j}(t' - t_1 - (l - l_1)\cos \Phi_j/\alpha) \end{aligned} \tag{A2}$$

where $r_{w_j}(t)$ is the autocorrelation of $w_j(t)$. Taking the sum with respect to j, we have

$$r'_{wx}(t'; l) = r_{wx}(t'; l) - m_1 r_w(t' - t_1 - (l - l_1)\cos \Phi_j/\alpha) \tag{A3}$$

where

$$\begin{aligned} r_{wx}(t'; l) &= \sum_j r_{w_j x_j}(t'; l) \\ r_w(t; l) &= \sum r_{w_j}(t - l \cos \Phi_j/\alpha). \end{aligned} \tag{A4}$$

REFERENCES

Abe, K. (1974). Seismic displacement and ground motion near a fault: the Saitama earthquake of September 21, 1931, *J. Geophys. Res.* **79,** 4393–4399.

Aki, K. (1968). Seismic displacement near a fault, *J. Geophys. Res.* **73,** 5359–5376.

Boatwright, J. (1980). Preliminary body-wave analysis of the St. Elias Alaska earthquake of February 28, 1979, *Bull Seism. Soc. Am.* **70,** 419–436.

Brune, J. N. (1970). Tectonic stress and spectra of seismic shear waves, *J. Geophys. Res.* **75,** 4997–5002.

Burdick, L. J. and G. R. Mellman (1976). Inversion of the body waves from the Borrego Mountain earthquake to the source mechanism, *Bull. Seism. Soc. Am* **66,** 1485–1499.

Chung, W.-Y. and H. Kanamori (1976). Source process and tectonic implications of the Spanish deep-focus earthquake of March 29, 1954, *Phys. Earth Planet. Interiors* **13,** 85–96.

Das, S. and K Aki (1977). Fault plane with barriers. a versatile earthquake model, *J. Geophys. Res.* **82,** 5658–5670.

Ebel, J. E. and D. V. Helmberger (1982). *P*-wave complexity and fault asperities· the Borrego Mountain, California, earthquakes of 1968, *Bull. Seism. Soc. Am.* **72,** 413–437.

Fukao, Y. (1972). Source process of a large deep-focus earthquake and its tectonic implications—The Western Brazil earthquake of 1963, *Phys. Earth Planet. Interiors* **5,** 61–76

Haskell, N. A. (1964). Total energy and energy spectral density of elastic wave radiation from propagating faults, *Bull. Seism. Soc. Am.* **54,** 1811–1841.

Haskell, N. A. (1969). Elastic displacements in the near-field of a propagating fault, *Bull. Seism. Soc. Am.* **59,** 865–908.

Imamura, A. (1937). *Theoretical and Applied Seismology*, Maruzen, Tokyo, 358 pp.

Jones, L. M. and P. Molnar (1979). Some characteristics of foreshocks and their possible relationship to earthquake prediction and premonitory slip on faults, *J. Geophys. Res.* **84,** 3596–3608.

Kanamori, H. (1972) Determination of effective tectonic stress associated with earthquake faulting, the Tottori earthquake of 1943, *Phys. Earth Planet. Interiors* **5,** 426–434.

Kanamori, H. (1981). The nature of seismicity patterns before large earthquakes, in *Earthquake Prediction*, W. Simpson and P. G. Richards, Editors, American Geophysical Union, Washington, D C., 1–19.

Kanamori, H and G. S. Stewart (1976). Mode of the strain release along the Gibbs fracture zone, Mid-Atlantic ridge, *Phys. Earth Planet. Interiors* **11,** 312–332.

Kanamori, H. and G. S. Stewart (1978). Seismological aspects of the Guatemala earthquake of February 4, 1976, *J. Geophys Res* **83,** 3427–3434.

Langer, C. J., J. P. Whitcomb, and A. Q. Aburto (1976). Aftershocks from local data, the Guatemalan earthquake of February 4, 1976, a preliminary report, *U S. Geol. Surv. Profess. Paper 1002*, 30–38.

Langston, C. A. (1976). A body wave inversion of the Koyna, India, earthquake of December 10, 1967, and some implications for body wave focal mechanisms, *J. Geophys Res.* **81,** 2517–2529.

Langston, C. A. and D. V. Helmberger (1975). A procedure for modelling shallow dislocation sources, *Geophys J.* **42,** 117–130.

Lay, T. and H. Kanamori (1981). An asperity model of great earthquake sequences, in *Earthquake Prediction*, D. W. Simpson and P. G Richards, Editors, American Geophysical Union, Washington, D.C., 579–592

Levinson, H. (1947) The Wiener RMS (root-mean-square) error criterion in filter design and prediction, *J. Math Phys*, 261–278.

Miyamura, S., S. Omote, R. Teisseyre, and E. Vesanen (1964). Multiple shocks and earthquake series pattern, *Int. Inst. Seismol. Earthquake Eng. Bull.* **2,** 71–92.

Plafker, G. (1976). Tectonic aspects of the Guatemala earthquake of 4 February 1976, *Science* **93,** 1201–1208.

Rial, J. A. (1978). The Caracas, Venezuela, earthquake of July 1967: a multiple-source event, *J. Geophys. Res.* **83,** 5405–5414

Strelitz, R. A. (1980). The fate of the downgoing slab a study of the moment tensors from body waves of complex deep-focus earthquakes, *Phys. Earth Planet. Interiors* **21,** 83–96.

Wesson, R. L and W. L. Ellsworth (1973). Seismicity preceding moderate earthquakes in California, *J. Geophys. Res.* **78,** 8527–8546.

Wyss, M. and J. N. Brune (1967). The Alaska earthquake of 28 March 1964: a complex multiple rupture, *Bull. Seism. Soc. Am.* **57,** 1017–1023.

SEISMOLOGICAL LABORATORY
CALIFORNIA INSTITUTE OF TECHNOLOGY
PASADENA, CALIFORNIA 91125

CONTRIBUTION NO. 3586

Manuscript received 15 June 1981